J|A|C|S
ARTICLES
Published on Web 02/22/2003

Photonic Crystal Carbohydrate Sensors: Low Ionic Strength Sugar Sensing

Sanford A. Asher,*,† Vladimir L. Alexeev,† Alexander V. Goponenko,† Anjal C. Sharma,† Igor K. Lednev,† Craig S. Wilcox,† and David N. Finegold‡

Contribution from the Department of Chemistry, Chevron Science Center, University of Pittsburgh, Pittsburgh, Pennsylvania 15260, and Department of Pediatrics, University of Pittsburgh Medical School, University of Pittsburgh, Pittsburgh, Pennsylvania 15260

Received July 30, 2002; E-mail: asher@pitt.edu

Abstract: We developed a carbohydrate sensing material, which consists of a crystalline colloidal array (CCA) incorporated into a polyacrylamide hydrogel (PCCA) with pendent boronic acid groups. The embedded CCA diffracts visible light, and the PCCA diffraction wavelength reports on the hydrogel volume. This boronic acid PCCA responds to species containing vicinal cis diols such as carbohydrates. This PCCA photonic crystal sensing material responds to glucose in low ionic strength aqueous solutions by swelling and red shifting its diffraction as the glucose concentration increases. The hydrogel swelling results from a Donnan potential due to formation of boronate anion; the boronic acid pK_a decreases upon glucose binding. This sensing material responds to glucose and other sugars at <50 μM concentrations in low ionic strength solutions.

Introduction

There is an ever-increasing demand for continuous, noninvasive glucose monitoring due to the increasing number of people diagnosed with *diabetes mellitus*[1] (type 1, insulin-dependent diabetes). The need for minimally invasive glucose sensing has also increased due to the recognition that the long-term health of diabetes mellitus patients is dramatically improved by careful glucose monitoring and control.[2] The development of accurate, reliable, continuous, and noninvasive glucose sensors would significantly improve the lives of diabetic patients and decrease their risk of hypoglycemia. These sensors would have to operate reliably at the physiological pH values and ionic strengths of bodily fluids and would have to be immune from interference by other species present.

This need for glucose sensors has motivated the investigation of numerous approaches, which were recently reviewed.[2] In the work here we describe a new photonic crystal carbohydrate sensing hydrogel material (PCCA, Figure 1) which can be used to detect sugars in low ionic strength solutions. This material consists of a polyacrylamide hydrogel with an embedded crystalline colloidal array (CCA). We previously demonstrated the use of this photonic crystal sensor motif to sense metal cations, pH, ionic strength, and glucose.[3−5]

Our previously demonstrated glucose sensor utilized glucose oxidase (GOD) as the molecular recognition element. The GOD conversion of glucose to gluconic acid reduced the GOD FAD prosthetic group, which became negatively charged. The formation of these covalently bound hydrogel anions resulted in a Donnan potential that resulted in an osmotic pressure that caused the hydrogel to swell, which red shifted the Bragg diffraction.[3,5] Unfortunately, the utility of this motif for measuring glucose was limited because it did not function at high ionic strength, its response depended upon the oxygen concentration (which reoxidized the FAD), and the accompanying production of hydrogen peroxide could be problematic for many applications.

We developed a new class of glucose sensing materials by attaching phenylboronic acid to our PCCA photonic crystal hydrogels. The use of boronic acid derivatives to sense, target, and separate diol-containing substances has been exploited for a long time (for recent reviews see refs 6 and 7). Polymers containing boronic acid groups are widely used for affinity purification.[8−10] Hydrogels with attached boronic acid moieties[11−15]

† Department of Chemistry.
‡ Department of Pediatrics.

(1) (a) Clark, C. M., Jr. *Diabetes Care* **1998**, *21* (Suppl. 3), C1−C2. (b) Davidson, M. B. *Diabetes Care* **1998**, *21*, 2152−2160.
(2) Pickup, J.; McCartney, L.; Rolinski, O.; Birch, D. *Br. Med. J.* **1999**, *319*, 1289−1293.
(3) Holtz, J. H.; Asher, S. A. *Nature.* **1997**, *389*, 829−832.
(4) Lee, K.; Asher, S. A. *J. Am. Chem. Soc.* **2000**, *122*, 9534−9537.
(5) Holtz, J. H.; Holtz, J. S. W.; Munro, C. H.; Asher, S. A. *Anal. Chem.* **1998**, *70*, 780−791.
(6) James, T. D.; Shinkai, S. *Top. Curr. Chem.* **2002**, *218*, 159−200.
(7) James, T. D.; Sandanayake, K. R. A. S.; Shinkai, S. *Supramol. Chem.* **1995**, *6*, 141−157.
(8) Hageman, J. H.; Kuehn, G. D. Boronic Acid Matrices for the Affinity Purification of Glycoproteins and Enzymes. In *Methods in Molecular Biology: Practical Protein Chromatography*; Kenney, A., Fowell, S., Eds.; The Human Press Inc.: Totowa, NJ, 1992; Vol. 11, Chapter 4, pp 45−71.
(9) Hageman, J. H.; Kuehn, G. D. *Anal. Biochem.* **1977**, *80*, 547−554.
(10) Maestas, R. R.; Prieto, J. R.; Kuehn, G. D.; Hageman, J. H. *J. Chromatogr.* **1980**, *189*, 225−231.
(11) Miyazaki, H.; Kikuchi, A.; Koyama, Y.; Okano, T.; Sakurai, Y.; Kataoka, K. *Biochem. Biophys. Res. Commun.* **1993**, *195*, 829−836.
(12) Kikuchi, A.; Suzuki, K.; Okabayashi, O.; Hoshino, H.; Kataoka, K.; Sakurai, Y.; Okano, T. *Anal. Chem.* **1996**, *68*, 823−828.
(13) Kanekiyo, Y.; Inoue, K.; Ono, Y.; Sano, M.; Shinkai, S.; Reinhoudt, D. N. *J. Chem. Soc., Perkin Trans. 2* **1999**, 2719−2722.

10.1021/ja021037h CCC: $25.00

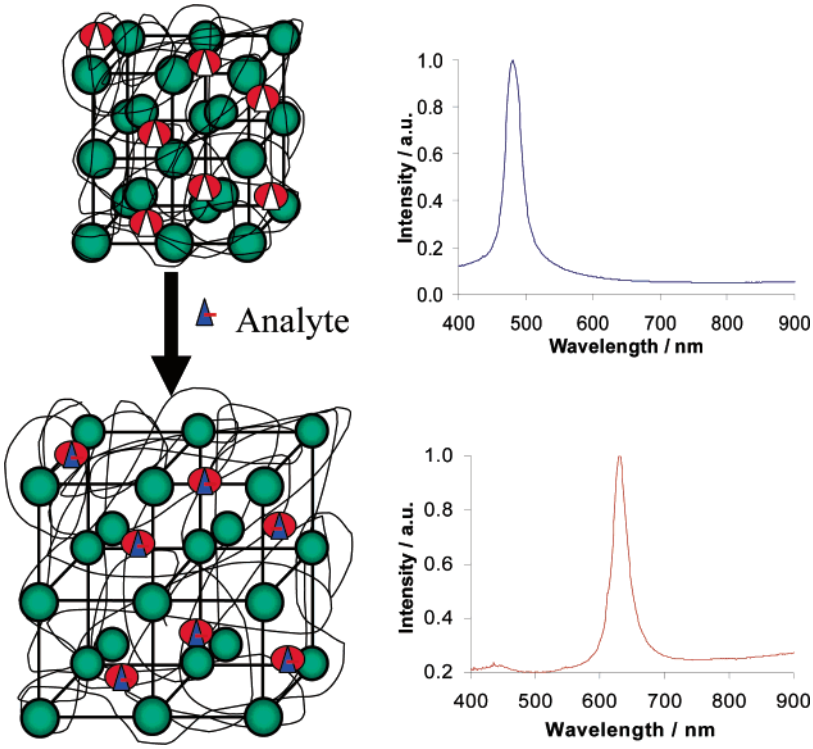

Figure 1. Polymerized crystalline colloidal array photonic crystal sensing materials consist of an embedded crystalline colloidal array (CCA) surrounded by a polymer hydrogel network which contains a molecular recognition element. The embedded CCA of polystyrene colloidal particles efficiently diffracts light of a wavelength determined by the array lattice constant. As shown by spectra on the right, diffracted wavelength red shifts result from hydrogel volume increases induced by the interaction of the analyte with the molecular recognition element.

have been used to bind cis diol-containing substances and lymphocytes. In addition, boronic acid derivatives have been polymerized in the presence of sugars to create imprinted sugar binding sites.[16−18]

Kikuchi et al.[12] previously demonstrated that polymer hydrogel volume changes could be actuated by boronic acid−sugar complexation. These hydrogel volume changes were utilized in a boronic acid−polymer membrane electrochemical detection scheme, where the hydrogel volume changes controlled ion diffusion to the electrode.[12] More recently, Arnold et al.[19] demonstrated an electrochemical conductometric glucose sensor that monitored the glucose concentration in whole blood and plasma. The detection scheme utilized the fact that glucose complexation to boronic acid releases protons and increases the local ionic strength.

Sugar-induced boronic acid hydrogel swelling was used in a quartz crystal microbalance sugar sensing study by the Shinkai group.[13,14] In fact, the Sakurai group[20,21] proposed that this glucose-induced boronic acid hydrogel swelling could be used for insulin delivery purposes.

Boronic acid derivatives have been synthesized that change their absorbance upon binding of cis diols.[22−25] For instance, Lavigne et al.[25] demonstrated a boronic acid-based colorimetric chemosensing ensemble to sense tartrate and malate. These derivatives can be utilized for colorimetric sugar sensing. In fact, boronic acid−sugar complexes can be used to control the pitch and resulting diffraction of a cholesteric liquid crystal.[26] It may be possible to design a detection scheme utilizing this approach.

Our PCCA photonic crystal glucose sensing hydrogel also utilizes color changes to report on sugar binding. These color changes result from shifts in the wavelength of Bragg diffracted light from the CCA incorporated into a hydrogel matrix. The PCCA volume depends on the concentration of bound sugars. These PCCA volume changes alter the CCA spacing, which alters the Bragg diffraction condition.[3−5]

This report is the first in a series of papers devoted to the use of boronic acids as molecular recognition elements in PCCA. Our objective is to utilize these photonic crystal glucose sensing materials for in vivo glucose sensors in the form of contact lenses to sense glucose concentration in a tear fluid or in the form of subcutaneous inserts to report glucose concentration in an interstitial fluid. In this publication we describe our first glucose sensing motif, which utilizes 3-aminophenylboronic acid as the molecular recognition agent. This carbohydrate sensor responds only in low ionic strength solutions. In subsequent papers we will describe a more sophisticated boronic acid complexation motif, which shows *selectivity* for glucose and is responsive at physiological pH values and ionic strengths.

(14) Kanekiyo, Y.; Sano, M.; Iguchi, R.; Shinkai, S. *J. Polym. Sci., Part A: Polym. Chem.* **2000**, *38*, 1302−1310.
(15) Gabai, R.; Sallacan, N.; Chegel, V.; Bourenko, T.; Katz, E.; Willner, I. *J. Phys. Chem. B* **2001**, *105*, 8196−8202.
(16) Wulff, G. *Pure Appl. Chem.* **1982**, *54*, 2093−2102.
(17) Glad, M.; Norrlöw, O.; Sellergren, B.; Siegbahn, N.; Mosbach, K. *J. Chromatogr.* **1985**, *347*, 11−23.
(18) Wulff, G. *Angew. Chem., Int. Ed. Engl.* **1995**, *34*, 1812−1832.
(19) Arnold, F. H.; Zheng, W.; Michaels, A. S. *J. Membr. Sci.* **2000**, *167*, 227−239.
(20) Kitano, S.; Koyama, Y.; Kataoka, K.; Okano, T.; Sakurai, Y. *J. Controlled Release* **1992**, *19*, 162−170.
(21) Shiino, D.; Murata, Y.; Kataoka, K.; Koyama, Y.; Yokoyama, M.; Okano, T.; Sakurai, Y. *Biomaterials* **1994**, *15*, 121−128.
(22) Davis, C. J.; Lewis, P. T.; McCarroll, M. E.; Read, M. W.; Cueto, R.; Strongin, R. M. *Org. Lett.* **1999**, *1*, 331−334.
(23) Koumoto, K.; Shinkai, S. *Chem. Lett.* **2000**, 856−857.
(24) Ward, C. J.; Patel, P.; Ashton, P. R.; James, T. D. *Chem. Commun.* **2000**, 229−230.
(25) Lavigne J. J.; Anslyn E. V. *Angew. Chem., Int. Ed.* **1999**, *38*, 3666−3669.
(26) James, T. D.; Harada, T.; Shinkai, S. *J. Chem. Soc., Chem. Commun.* **1993**, 857−860.

Scheme 1. Two Routes to Chemically Modify the PCCA Hydrogel Backbone

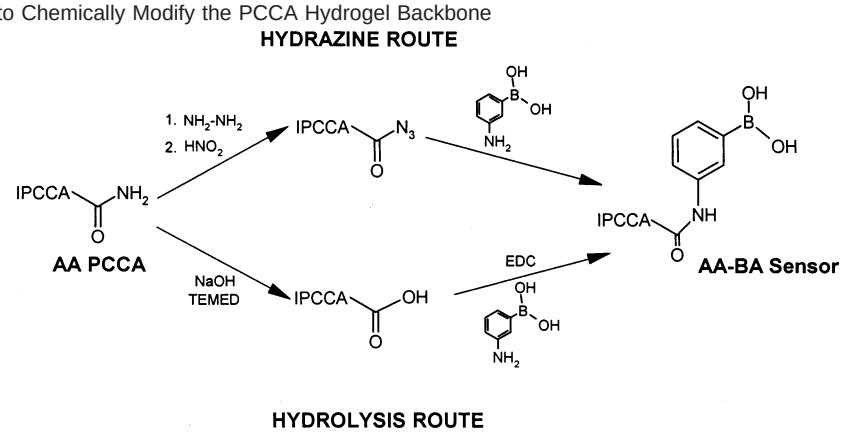

Experimental Section

β-D-(+)-Glucose, methyl-α-D-glucopyranoside, D-(+)-mannose, D-(−)-fructose, and D-(+)-galactose were purchased from Sigma and were used as received. Tris-HCl (enzyme grade, supplied from USB, USA), NaCl (J. T. Baker), 2,2-diethoxyacetophenone (DEAP, Acros Organics), acrylamide (AA, Fluka), *N*,*N*′-methylenebisacrylamide (bisAA, Fluka), 3-aminophenylboronic acid hemisulfate (BA, Acros Organics), 3-acetamidophenylboronic acid (Combi-Blocks Inc., USA), hydrazine (Aldrich), $NaNO_2$ (Fluka), HCl (J. T. Baker), NaOH (J. T. Baker), *N*,*N*,*N*′,*N*′-tetramethylethylenediamine (TEMED, Aldrich), and 1-[3-(dimethylamino)propyl]-3-ethylcarbodiimide hydrochloride (EDC, Aldrich) were used as received. Diffraction from the sensing materials was measured by using a SI 400 (model 430/440) diode array spectrometer (Spectral Instruments, USA). UV spectra were measured by using a Perkin-Elmer Lambda 9 UV/vis/NIR spectrometer.

Preparation of CCAs. Highly charged monodisperse polystyrene colloids were prepared by emulsion polymerization as described elsewhere.[27] We used 5−10 wt % suspensions of ∼140 nm polystyrene colloidal particles. The suspensions were cleaned by dialysis against deionized water (17.5 MΩ·cm^{-1}, Barnstead Nanopure Water Purification System) and by shaking with ion-exchange resin. The suspension became iridescent due to Bragg diffraction from the CCA upon shaking with ion-exchange resin. Each particle possesses ∼40 000 strong ionizable acid groups.

Preparation of AA-PCCA. The PCCAs were synthesized by a free radical solution polymerization which utilized DEAP as a photoinitiator. A typical recipe utilized 100 mg (1.4 mmol) of AA, 5 mg (33.7 μmol) of bisAA, 2 g of the CCA suspension (8−10 wt %) in deionized water, and ∼50 mg of ion-exchange resin. This polymerization mixture was shaken for 10−15 min and deoxygenated by nitrogen bubbling. A 7.7 μL sample of a 10% solution of DEAP in DMSO (3.84 μmol of DEAP) was added to the AA−bisAA−CCA suspension, and the solution was shaken for an additional 10 min and then centrifuged for 30 s to precipitate the resin particles. This dispersion was injected into a cell consisting of two clean quartz disks separated by either a 125 μm Parafilm film or by two 40 μm Duraseal spacers.

Photopolymerization was performed using UV mercury lamps [Black Ray (365 nm)] for 40−60 min. The cells were opened and the PCCAs were washed overnight in copious amounts of distilled water. If all of the bisacrylamide formed *effective*[28] hydrogel cross-links, the stoichiometry would yield a ∼0.03 M cross-link density. In contrast, the elastic measurements of Lee and Asher[4] indicate a much smaller *effective* cross-link density of ∼1.5 mM.

Chemical Modification of Hydrogel Backbone. The synthetic procedures are shown in Scheme 1.

1. Azide Route. The PCCA hydrogel backbone was functionalized with acyl azide groups to facilitate the attachment of 3-aminophenylboronic acid. The hydrazine treatment was performed as previously described.[29−31] The PCCA was immersed in 25 mL of a 6 M aqueous hydrazine solution at 47 °C for 1 h to generate PCCA-containing acyl hydrazine side chains. After repeated washing with 0.1 M aqueous NaCl and with cold water, the gel was immersed for 20 min in a cold aqueous nitrous acid solution formed by mixing 32 mL of 0.25 M HCl with 10 mL of 1 M $NaNO_2$. This hydrazine treatment should also convert some (<2%) of the amides to carboxyl groups.[29,31]

The resulting acyl azide gel was then repeatedly washed with 0.1 M NaCl and cold water. We attached BA by immersing the acyl azide-functionalized PCCA in a 0.2 M 3-aminophenylboronic acid solution (pH 8.5) in an ice bath for 1−2 days. The remaining azide groups were removed by treating the IPCCA with 0.1 M NH_4OH for 20 min.[30]

2. Hydrolysis Route. Another route to the AA−BA PCCA involves hydrolysis of the PCCA amide groups. The PCCAs were placed in a 0.1 N NaOH solution containing 10% v/v TEMED for 1.5−2 h. The hydrolyzed PCCAs were then extensively washed with water and immersed in a solution containing 25 mM EDC and 25 mM 3-aminophenylboronic acid for 2−4 h, to obtain the AA−BA PCCA. These PCCAs were repeatedly washed with distilled water.

Because of carboxyl ionization, the washed hydrolyzed gels extensively swell in water and diffract in the IR region. The gel diffraction after BA attachment returned almost to that of the original nonhydrolyzed PCCA, indicating that most of the carboxyl groups formed amide bonds with BA. Atomic emission determination of the boron content (Desert Analytics Co.) indicates that our procedure incorporates 0.27 mmol of BA per g of dry PCCA.

Results

Figure 2 shows the glucose concentration dependence of diffraction of the phenylboronic acid PCCA sensor in 2 mM Tris buffer at pH 8.5. The spectral peaks derive from diffraction of normally incident light by the fcc 111 planes of the embedded CCA.[3−5] In the absence of glucose the sensor shows a symmetric diffraction peak at 496 nm, indicating that it diffracts blue-green light. This diffraction peak red shifts as the glucose concentration increases; the sensor diffracts green light at 506 nm for 1 mM glucose, orange light at 576 nm for 20 mM glucose, and red light at 624 nm for 100 mM glucose, for example. Thus, this sensor responds to glucose by changing its diffraction wavelength; the color changes are visually evident and can be used to visually estimate the glucose concentration.

(27) Reese, C. E.; Guerrero, C. D.; Weissman, J. M.; Lee, K.; Asher, S. A. *J. Colloid Interface Sci.* **2000**, *232*, 76−80.
(28) Flory, P. J. *Principles of Polymer Chemistry*; Cornell University Press: Ithaca, NY, 1953.
(29) Inman, J. R.; Dintzis, H. M. *Biochemistry* **1969**, *8*, 4074−4082.
(30) Weith, H. L.; Wiebers, J. L.; Gilham, P. T. *Biochemistry* **1970**, *9*, 4396−4401.
(31) Inman, J. K. Covalent Linkage of Functional Groups, Ligands, and Proteins to Polyacrylamide Beads. In *Methods in Enzymology*; 1974; Vol. 34, Chapter 3, pp 30−58.

Scheme 2. Equilibria Associated with 3-Acetamidophenylboronic Acid Glucose Binding

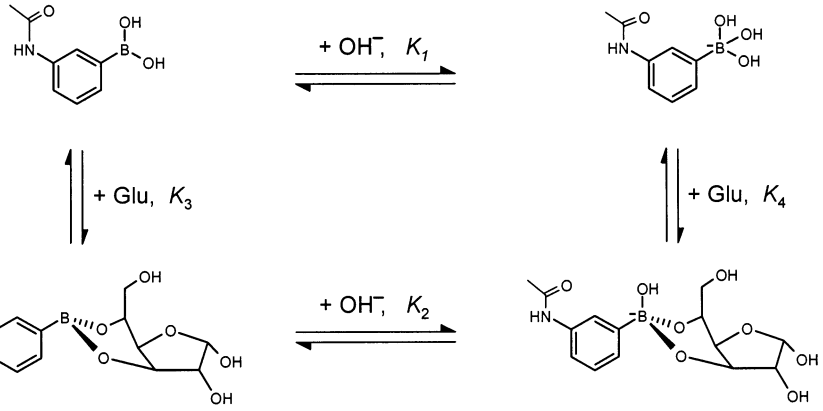

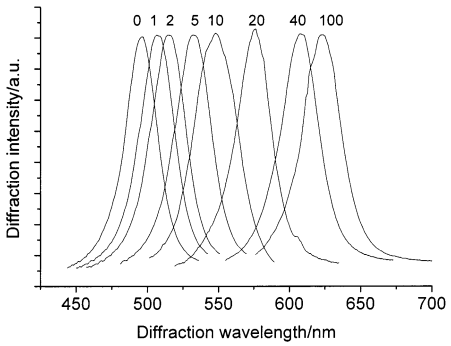

Figure 2. Glucose concentration dependence of diffraction of the boronic acid PCCA sensor in 2 mM Tris-HCl buffer at pH 8.5. The diffraction peaks are labeled with their glucose concentrations (mM).

The response of the sensor to glucose decreases upon addition of NaCl and ceases for NaCl concentrations greater than 10 mM. In addition, the sensor response decreases for pH values below pH = 8.5; the sensor becomes unresponsive to glucose at pH < 7. The sensor swells as the pH increases to pH 9.5 because all of the boronic acids titrate to boronates. Thus, the sensor becomes unresponsive to glucose at pH > 9.5.

We examined the dependence of the diffraction wavelength on glucose concentration in distilled water and found a detection limit of approximately 50 μM for the sensors described herein. We can readily decrease the detection limit by decreasing the hydrogel cross-linking or increasing the concentration of boronic acid groups.[3−5]

The glucose-induced diffraction red shifts originate from hydrogel swelling due to the formation of anionic boronate groups upon glucose binding (Scheme 2); the pK_a of phenylboronic acid derivatives drops upon diol binding[6,7,19,32−39] (also see Appendix). The diffracted wavelength changes linearly with changes in the embedded fcc 111 plane CCA lattice constant, which varies as the 1/3 power of the hydrogel volume.

Figure 3 shows the concentration dependence of the linear deformation factor, $\alpha = \lambda/\lambda_o = (V/V°)^{1/3}$, for this PCCA for glucose, fructose, mannose, galactose, and methyl-α-D-glucopyranoside, where V is the equilibrium volume of the PCCA at the defined sugar concentration and $V°$ is the volume in the absence of the sugar. All of the sugars increase the PCCA linear deformation factor as their concentrations increase. The responses of these sensors are fully reversible; decreases in the sugar concentration blue shift the diffraction. The maximum red shift occurs for fructose, which has the largest K_4 association constant. The other sugars have significantly lower boronate K_4 association constants and different K_3 boronic acid association constants[32] (Table 1).

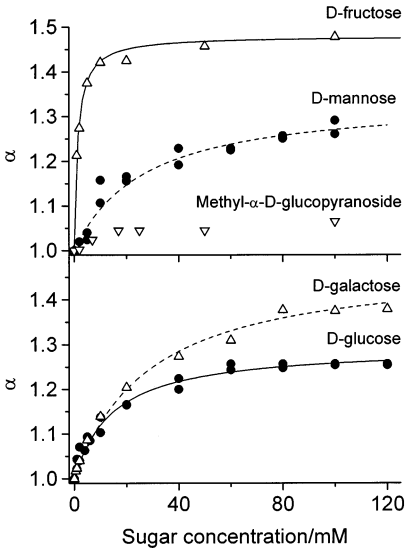

Figure 3. D-Glucose, D-fructose, D-mannose, D-galactose, and methyl-α-D-glucopyranoside concentration dependence of the linear deformation factor, $\alpha = \lambda/\lambda_o = (V/V°)^{1/3}$, for this PCCA. The solid lines are fits to the theoretical model as discussed in the text. We were unable to find a published value for the association constant of methyl-α-D-glucopyranoside to phenylboronic acid derivative.

Discussion

The glucose-induced PCCA diffraction shift results from formation of anionic boronate−glucose complexes, which are covalently linked to the PCCA hydrogel. At low ionic strengths significant differences can occur between the concentrations of ions in the PCCA and in the surrounding sample solution. This difference results in a Donnan potential that forces the gel to swell and the diffraction to red shift.[3−5] As shown by the solid lines in Figure 3, we successfully modeled the PCCA response to sugars by improving our previous model for ionic PCCA swelling[4] that was based on the earlier work of Flory.[28]

(32) Lorand, J. P.; Edwards, J. O. *J. Org. Chem.* **1959**, *24*, 769−774.
(33) Sienkiewicz, P. A.; Roberts, D. C. *J. Inorg. Nucl. Chem.* **1980**, *42*, 1559−1575.
(34) Singhal, R. P.; DeSilva, S. S. M. *Adv. Chromatogr.* **1992**, *31*, 293−335.
(35) Singhal, R. P.; Ramamurthy, B.; Govindraj, N.; Sarwar, Y. *J. Chromatogr.* **1991**, *543*, 17−38.
(36) Soundararajan, S.; Badawi, M.; Kohlrust, C. M.; Hageman, J. H. *Anal. Biochem.* **1989**, *178*, 125−134.
(37) James, T. D.; Linnane, P.; Shinkai, S. *Chem. Commun.* **1996**, 281−288.
(38) Yoon, J.; Czarnik, A. W. *J. Am. Chem. Soc.* **1992**, *114*, 5874−5875.
(39) James, T. D.; Sandanayake, K. R. A. S.; Shinkai, S. *Angew. Chem., Int. Ed. Engl.* **1994**, *33*, 2207−2209.

Table 1. Sugar Binding Equilibrium Constants to Boronic Acid Derivatives and to the Boronic Acid Derivative Bound to the PCCA

sugar	PCCA K_3/M^{-1}	K_3/M^{-1}	PCCA K_4/M^{-1}	K_4/M^{-1}
fructose	<10		2000	4370[a]
mannose	12		90	172[a]
glucose	28	< 1[b]	150	600[b]
				50−160[a]
				630[c]
galactose	<1		100	276[a]

[a] For 3-aminophenylboronic acid in solution by Lorand et al.[32] [b] For 3-acetamidophenylboronic acid in solution as measured here. [c] Phenylboronic acid attached by an amide linkage at the 3-position to an acrylamide hydrogel.[21]

The equilibrium volume of our PCCA is determined by the condition that the total hydrogel osmotic pressure $\Pi_T = 0$. The total osmotic pressure is the sum of the osmotic pressures due to the free energy of mixing, Π_M, the hydrogel network elastic restoring force, Π_E, and the osmotic pressure associated with the mobile ion concentration inside and outside the gel, Π_{ion} (Donnan potential): $\Pi_T = \Pi_M + \Pi_E + \Pi_{Ion}$, where

$$\Pi_M = -\frac{\partial \Delta G_M}{\partial V} = -\frac{RT}{V_s}\left[\ln\left(1-\frac{V_0}{V}\right)+\frac{V_0}{V}+\chi\left(\frac{V_0}{V}\right)^2\right] \quad (1)$$

$$\Pi_E = -\frac{\partial \Delta G_E}{\partial V} = -\frac{RT\cdot n_{cr}}{V_m}\left[\left(\frac{V_m}{V}\right)^{1/3}-\frac{1}{2}\frac{V_m}{V}\right] \quad (2)$$

$$\Pi_{Ion} = RT(c_+ + c_- - c_+^* - c_-^*) \quad (3)$$

where R is universal gas constant, T is the temperature, χ is the Flory−Huggins interaction parameter for the polymer network and the solution, V_s is the molar volume of the solvent, n_{cr} is the effective number of cross-linked chains in the network, V is the existing volume of the gel, V_m is the volume of the relaxed network, V_0 is the volume of the dry polymer network, c_+ and c_- are the concentrations of mobile cations and anions inside the gel, and c_+^* and c_-^* are the concentrations outside the gel. In the case here we use the simplifying conditions that all ionic species are singly charged and the anion/cation stoichiometry is unity.

We utilize the crucial assumptions[4] that the hydrogel polymerization occurred under conditions where the cross-linked chain length distribution is in its statistically most probable configuration(s) such that the volume of the prepared gel (before washing) is equal to V_m. We utilize the hydrogel cross-link density obtained previously ($n_{cr}/V_m = 1.46 \times 10^{-3}$ M) and the Flory−Huggins interaction parameter $\chi = 0.49$ for polyacrylamide.[40]

As elaborated by Flory,[28] the concentration of ions inside the gel can be calculated by utilizing the requirement of electroneutrality in the gel and by equating the product of the activities of the ions inside and outside the gel. Thus, if the system contains only monovalent ions, the difference between concentrations of mobile anions and cations in the gel will be equal to the charge covalently attached to the polymer network.

We expect that the only ionic species bound to the gel are the phenylboronates: $c_+ = c_B + c_{BG} + c_s$ and $c_- = c_s$, where c_B and c_{BG} are the concentrations of the phenylboronate anion and of the phenylboronate−glucose anion complex attached to the gel. c_s is the electrolyte concentration in the gel. The concentrations of boronate species were calculated from the reactions of Scheme 2 (see details in the Appendix) taking into account the pH within the gel (which due to the Donnan potential differs from the pH of the external solution). We also include the boronic acid concentration changes due to hydrogel volume changes.

The pH inside the gel was calculated by recognizing that identical water activities in the gel and in the reservoir require that $[H^+][OH^-] = [H^+]^*[OH^-]^*$ and that the other electrolyte activities (electrolyte $CA = C^+ + A^-$) must be identical inside and outside the gel. Assuming that ion activities are equal to concentrations, the equality of the chemical potential of the electrolytes requires that the products of concentration of cations and anions inside and outside the gel be equal:

Since $c_+^* = c_-^*$ we will define $c_+^* = c_-^* = c_s^*$ and $c_+ \cdot c_- = c_+^* \cdot c_-^*$

Further, $[H^+]/[H^+]^* = c_s^*/c_s$ and $\Pi_{Ion} = RT(c_B + c_{BG} - 2(c_s^* - c_s))$ (4)

Since the diffraction wavelength λ_D is directly proportional to $V^{1/3}$, solving the set of eqs 1, 2, and 4 for the value of V for which $\Pi_T = 0$ determines the dependence of the diffracted wavelength on the glucose concentration, provided that we know the solution electrolyte concentration and the ionization equilibria of the boronic acid species. The electrolyte concentrations are determined by the 2 mM Tris buffer equilibrium at the pH = 8.5 conditions used and the extent of boronic acid ionization. The charge covalently bound to the gel is determined by the glucose-dependent boronic acid−boronate ionization equilbria.

An extensive body of literature exists on the mechanism of carbohydrate−phenylboronic acid complexation.[6,7,19,41−47] The equilibria are extraordinarily complex due to the multiple sugar conformations in solution and due to the fact that binding can be bis-bidentate for sugars with multiple cis diols. Even in the simplest case four different species may occur in the glucose binding equilibrium (Scheme 2).

We are able to successfully model the dependence of the diffraction wavelength on the sugar concentration (Figure 3) by utilizing eqs 1, 2, and 4, by assuming the simple sugar binding equilibria of Scheme 2 and by fitting for the sugar binding equilibrium constants (Table 1).

The values calculated from fitting differ somewhat from those measured for phenylboronic acid derivatives in solution. To compare the values for glucose, we (re)measured the equilibrium glucose binding constants and pK_a values for 3-acetamidophenylboronic acid and 3-aminophenylboronic acid (Appendix).

We find that the K_4 equilibrium binding value found for PCCA boronate glucose binding is 4-fold smaller than to 3-acetamidophenylboronic acid in solution as well as bound to

(40) Janas, V. F.; Rodriguez, F.; Cohen, C. *Macromolecules* **1980**, *13*, 977−983.
(41) James, T. D.; Sandanayake, K. R. A. S.; Shinkai, S. *Angew. Chem., Int. Ed. Engl.* **1996**, *35*, 1911−1922.
(42) Norrild, J. C.; Eggert, H. *J. Am. Chem. Soc.* **1995**, *117*, 1479−1484.
(43) Norrild, J. C.; Eggert, H. *J. Chem. Soc., Perkin Trans. 2* **1996**, 2583−2588.
(44) Bielecki, M.; Eggert, H.; Norrild, J. C. *J. Chem. Soc., Perkin Trans. 2* **1999**, 449−455.
(45) Eggert, H.; Frederiksen, J.; Morin, C.; Norrild, J. C. *J. Org. Chem.* **1999**, *64*, 3486-3846.
(46) Norrild, J. C. *J. Chem. Soc., Perkin Trans. 2* **2001**, 719−726.
(47) Uggla, R.; Sundberg, M. R.; Nevalainen, V. *Acta Chem. Scand.* **1999**, *53*, 34−40.

the acrylamide hydrogel of Shiino et al.[21] In contrast, the K_3 value for boronic acid glucose binding is much larger than for 3-acetamidophenylboronic acid in solution. These differences may result from the different environment of the phenylboronic acid moieties in the PCCA and because some of the boronate binding sites may not be accessible to glucose in the PCCA. In addition, the effective boronic acid pK_a may be higher in our PCCA.

Conclusions

We developed a photonic crystal hydrogel carbohydrate sensing material, which consists of a polyacrylamide hydrogel PCCA with pendent boronic acid groups. This material responds to sugars in low ionic strength aqueous solutions by red shifting its diffraction as the sugar concentration increases. This swelling of the hydrogel network results from an osmotic pressure generated by boronic acid ionization due to the boronic acid pK_a decrease caused by glucose binding. We quantitatively modeled the response of our carbohydrate sensor to various sugars by extending hydrogel volume phase transition theory. The color of these sensors can be visually evaluated to determine sugar concentration.

This sensing motif does not operate in high ionic strength solution since the Donnan potential becomes swamped at high ion concentrations. In a subsequent publication we will describe another boronic acid PCCA sensor that is selective for glucose and operates at high ionic strength that may prove useful for development of noninvasive or minimally invasive in vivo glucose sensors for patients with diabetes mellitus.

Appendix

We determined the equilibrium constants shown in Scheme 2 for phenylboronic acid, 3-acetamidophenylboronic acid, and 3-aminophenylboronic acid in aqueous solution by examining the pH dependence of their absorption spectra (Figure 4). All derivatives show absorption bands between 190 and 325 nm which derive from the perturbed transitions of the benzene aromatic rings. The high pH 257 nm phenylboronate band (Figure 4), which has the low molar absorptivity of $\epsilon_{max} \approx 200$ M^{-1} cm^{-1}, characteristic of the forbidden substituted benzene L_b transition, shows the characteristic vibronic progression of the benzenoid symmetric ring breathing vibration at $\sim$900 cm^{-1} in the excited state.[48] Formation of the phenylboronic acid at lower pH doubles the oscillator strength and red shifts this band by $\sim$9 nm (Figure 4A). A much larger change occurs for the phenylboronate L_a band, which appears as a shoulder at 207 nm and red shifts to 217 nm in the phenylboronic acid form. Obviously the boronate and boronic acid aromatic ring substituents only weakly perturb the aromatic ring excited state structure and boronic acid is more perturbing than boronate.

Dramatic absorption spectral changes occur upon amide or amine substitution in 3-acetamidophenylboronic acid (Figure 4B) and 3-aminophenylboronic acid (Figure 4C and D), which indicates significantly stronger benzene ring electronic transition perturbations. The spectra resemble those substituted derivatives such as cresolate, for example.[48] The weak L_b bands red shift out to 260−300 nm, while the stronger L_a bands shift to $\sim$240 nm. The fully allowed benzenoid $B_{a,b}$ bands shift down to just above 200 nm.

(48) Asher, S. A.; Ludwig, M.; Johnson, C. R *J. Am. Chem. Soc*. **1986**, *108*, 3186−3197.

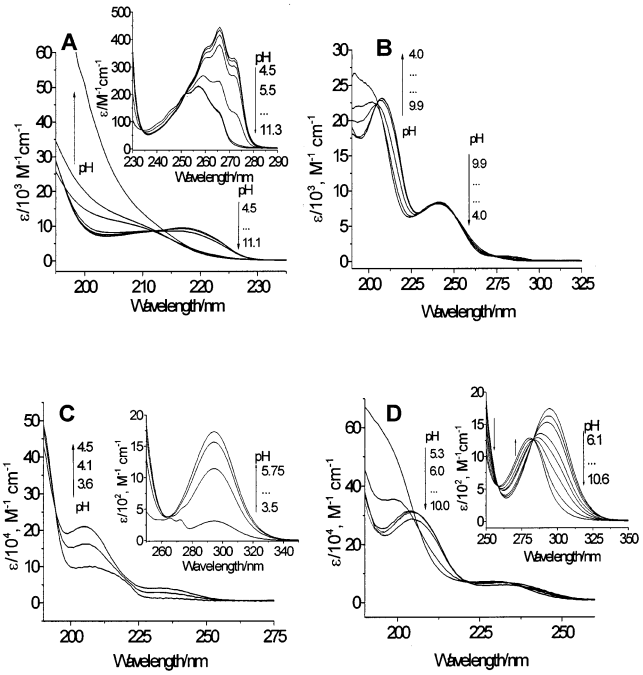

Figure 4. pH dependence of absorption spectra of phenylboronic acid derivatives (1 cm path length). (A) 0.05 mM phenylboronic acid aqueous solution at pH 4.5, 5.7, 7.8, 8.3, 9.7, 10.3, and 11.1 Inset: 1 mM phenylboronic acid aqueous solutions at pH 4.5, 5.5, 6.9, 7.7, 8.6, 10.3, and 11.3. (B) 0.05 mM 3-acetamidophenyl boronic aqueous solutions at pH 4.0, 5.5, 7.5, 8.4, 9.0, and 9.9. (C) 1 μM 3-aminophenyl boronic acid aqueous solutions at pH 3.6, 4.1, and 4.5. Inset: 1 mM at pH 3.5, 4.5, 5.1, and 5.75. (D) 1 μM 3-aminophenyl boronic acid aqueous solutions at pH 5.3, 6.0, 6.9, 7.8, 9.0, and 10.0. Inset: 1 mM 3-aminophenyl boronic acid aqueous solutions at pH 6.1, 7.6, 7.9, 8.5, 8.7, 9.0, 9.6, and 10.6.

Scheme 3. Equilibria between Neutral and Charged 3-Aminophenylboronic Acid

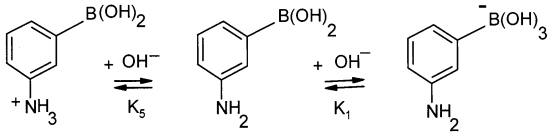

The low pH 3-acetamidophenylboronic acid weak L_b band at $\sim$285 nm appears to blue shift into a shoulder of the high pH 9.9 acetamidophenylboronate derivative (Figure 4B). Little change occurs in the strong 240 nm L_a band, while the higher energy 207 nm $B_{a,b}$ band of 3-acetamidophenylboronate red shifts $\sim$5 nm in the boronic acid derivative.

3-Aminophenylboronic acid (Figure 4C and D) shows a much richer pH spectral dependence since both the boronic acid and the amine substituents ionize (Scheme 3). The lowest pH absorption spectrum of 3-aminophenylboronic acid shows a very weak L_b-like absorption at $\sim$265 nm with $\epsilon_{max} < 300$ M^{-1} cm^{-1} with vibronic fine structure. This indicates little perturbation of the electronic structure of the aromatic ring by the protonated amine and boronic acid substituents. In contrast, as the pH increases, the amine deprotonates and a much stronger 294 nm absorption L_b band appears ($\epsilon_{max} \approx 1700$ $M^{-1}cm^{-1}$) with an L_a band at $\sim$240 nm and the $B_{a,b}$ band at $\sim$205 nm. Thus, the amine substituent significantly perturbs the electronic structure. Formation of the boronate at higher pH significantly blue shifts each band.

The pH absorption titrations show clear isosbestic points indicating simple titration behaviors except at the highest pH values below 220 nm, where the absorption of the OH^- interferes. Figure 5 shows the pH dependence of absorbance of

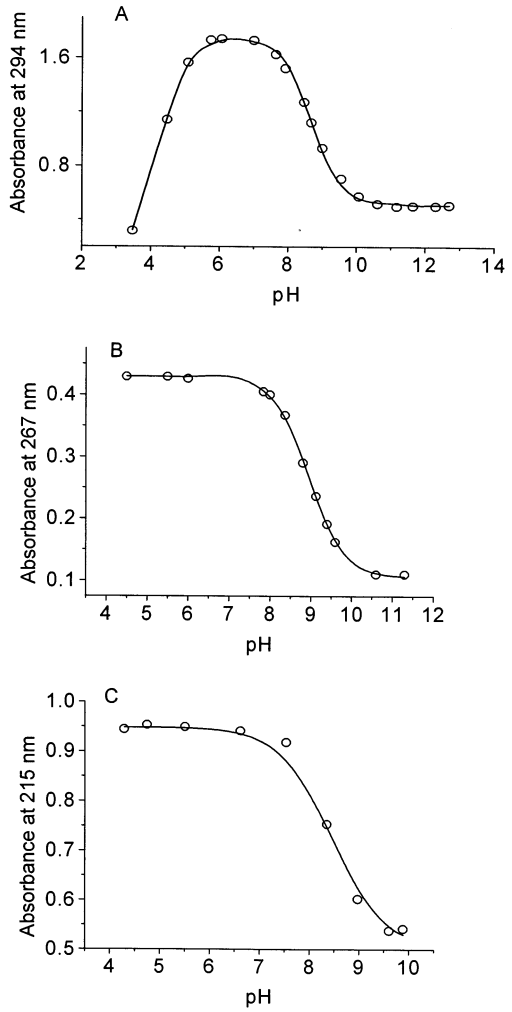

Figure 5. pH-dependence of the UV-absorbance of (A) 1 mM 3-aminophenylboronic acid aqueous solution at 294 nm, (B) 1 mM phenylboronic acid aqueous solution at 267 nm, (C) 0.05 mM 3-acetamidoboronic acid aqueous solution at 215 nm.

each derivative at wavelengths most sensitive to the spectral changes. Equation 5 was used to fit the phenylboronic acid and the 3-acetamidophenylboronic absorbance pH dependencies.

$$A = A_\infty + \frac{A_0 - A_\infty}{1 + K_1 \cdot [\mathrm{OH}]} \tag{5}$$

where A_0 and A_∞ are the absorbances at low and high pH, respectively. Equation 6 was used to fit the 3-aminophenylboronic acid absorbance pH dependence in order to include all three species involved in the pH equilibria (Scheme 3).

$$A = 2A_2 - A_3 + \frac{\{A_1 - 2A_2 + A_3 + (A_3 - A_2) \cdot K_5[\mathrm{OH}]\} \cdot (1 + 2K_1[\mathrm{OH}])}{1 + K_5[\mathrm{OH}] + K_5K_1[\mathrm{OH}]^2 + 2K_1[\mathrm{OH}]} \tag{6}$$

A_1 and A_2 are the absorbances of the protonated and the deprotonated amine forms of acid, while A_3 is the absorbance of the boronate form, respectively; K_5 and K_1 are equilibrium constants for reactions 1 and 2 in Scheme 3; $[\mathrm{OH}] = 10^{\mathrm{pH}-14}$ is the concentration of hydroxyl ions.

From the pH dependence of the phenylboronic acid absorbance at 267 nm (Figure 5) we determined the phenylboronic acid $pK_a = 8.9 \pm 0.1$, which is identical to the 8.86 value measured by direct titration[49] in the 1930s. The 3-aminophenylboronic acid pK_a value for the boronic acid group is calculated to be 8.37 ± 0.05, while the pK_a for protonation of the 3-aminophenylboronic acid amine is calculated to be 4.52 ± 0.09. This pK_a value for amine protonation agrees well with previous data, while our pK_a 8.37 boronic acid ionization value is significantly below the 8.75 value previously reported.[35] The difference appears to result from the use of an approximate model for the pH equilibrium that separately calculates the pK_a values for the low pH and high pH titrations by assuming equilibria between only two species. Our high pH and low pH data when separately modeled also yield a $pK_a = 8.7$. We determined a 3-acetamidophenylboronic acid of $pK_a = 8.5 \pm 0.1$, which is identical to the previously reported value.[21]

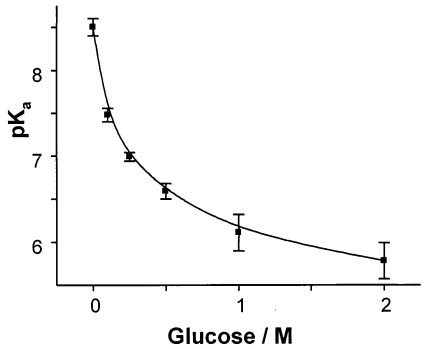

Figure 6. Glucose concentration dependence of the apparent pK_a value for hydroxylation of 3-acetamidophenylboronic acid. The solid line is a theoretical best fit of the data (see text for details).

To model the pH dependence of our PCCA glucose response, we require the equilibrium binding constants of the bound boronic acid derivatives, as well as the pK_a values of the glucose−BA complexes. It is already well documented that the pK_a of boronic acid drops upon cis diol binding.[6,7,19,32−39] Figure 6 shows the apparent pK_a values of 3-acetamidophenylboronic acid as measured by absorption spectral titrations at different glucose concentrations. As expected, the apparent pK_a decreases as the glucose concentration increases.

We utilized eq 7 and 8 to determine the equilibrium binding constants.

$$A = A_\infty + \frac{A_0 - A_\infty}{1 + K^* \cdot [\mathrm{OH}]} \tag{7}$$

$$K^* = \frac{K_1 + K_3K_2[\mathrm{G}]}{1 + K_3[\mathrm{G}]} \tag{8}$$

where K^* is the effective equilibrium constant for formation of the boronate complexes, which is a function of glucose concentration, [G].

We can independently calculate three equilibrium constants: $K_1 = 3.2 \times 10^5\ \mathrm{M}^{-1}$ ($pK_a = 8.5$), $K_2 > 2 \times 10^8\ \mathrm{M}^{-1}$ ($pK_a < 5.7$), and $K_3 < 1\ \mathrm{M}^{-1}$. Using the upper and lower limit values yields $K_4 = K_2K_3/K_1 \approx 600\ \mathrm{M}^{-1}$, which is essentially identical to the previously reported value[21] of $630\ \mathrm{M}^{-1}$ for the glucose binding affinity of phenylboronates bound through an amide linkage at the 3-position to an acrylamide hydrogel. Thus, the

(49) Branch, G. E. K.; Yabroff D. L.; Bettman B. *J. Am. Chem. Soc.* **1934**, *56*, 937−941.

stability constant for the boronate complex is greater by 600-fold compared to the boronic acid complex. To the best of our knowledge, these are the first measurements of K_3 value for neutral phenylboronic acid glucose binding.

Similar measurements of 3-aminophenylboronic acid gives $K_1 = 2 \times 10^5\ M^{-1}$ ($pK_a = 8.7$), $K_2 = 1.6\ X\ 10^8\ M^{-1}$ ($pK_a = 5.8$), and $K_3 \approx 0.1\ M^{-1}$. This yields a $K_4 = 80\ M^{-1}$, a value within Lorand et al.'s[32] range of $50-160\ M^{-1}$. Lorand et al.'s values[32] were determined by direct titration.

Acknowledgment. We gratefully acknowledge financial support from NIH grant DK55348 and ONR grant N00014-94-1-0592. We wish to gratefully acknowledge Dr. Sasmita Das for her help and Professor Rex Shepherd for valuable discussions on the mechanism of glucose boronate bonding. We are also grateful to Chad Reese, who generously supplied us with abundant amounts of colloid.

JA021037H